J. Biochem. 2009;145(3)315–324
doi:10.1093/jb/mvn166

Characterization of Moloney Murine Leukaemia Virus/Avian Myeloblastosis Virus Chimeric Reverse Transcriptases

Kiyoshi Yasukawa*, Masaki Mizuno and Kuniyo Inouye

Division of Food Science and Biotechnology, Graduate School of Agriculture, Kyoto University, Sakyo-ku, Kyoto 606-8502, Japan

Received November 19, 2008; accepted December 1, 2008; published online December 6, 2008

Reverse transcriptases (RTs) from Moloney murine leukaemia virus (MMLV) and avian myeloblastosis virus (AMV) contain all the fingers, palm, thumb, connection and RNase H domains. The fingers, palm and thumb domains are thought to be involved in the reverse transcription activity, and the RNase H domain is in the RNase H activity. In this study, we characterized four chimeric RTs which comprise one of the fingers, palm, thumb and RNase H domains originated from AMV RT and the other three and connection domains originated from MMLV RT. Unexpectedly, all chimeric RTs exhibited the same characteristics: their specific reverse transcription activities decreased to less than 0.1% of that of MMLV RT, while their specific RNase H activities were approximately 20% of that of MMLV RT. The decreases in the two activities of the chimeric RTs were ascribed to the decreases in k_{cat}. Based on that the reverse transcription activity of MMLV RT was impaired by substituting its RNase H domain with that from AMV RT, we propose that in MMLV RT, there might be an interaction between the fingers/palm/thumb domain and the RNase H domain.

Key words: avian myeloblastosis virus, chimeric enzyme, Moloney murine leukaemia virus, reverse transcriptase, RNase H.

Abbreviations: AMV, avian myeloblastosis virus; MMLV, Moloney murine leukaemia virus; RT, reverse transcriptase; T/P, template–primer; TCA, trichloroacetic acid.

INTRODUCTION

Reverse transcriptase (RT) [EC 2.7.7.49] is the enzyme responsible for viral genome replication, possessing RNA- and DNA-dependent DNA polymerase and RNase H activities (*1*, *2*). RTs from Moloney murine leukaemia virus (MMLV) and avian myeloblastosis virus (AMV) have been the most extensively used in cDNA synthesis (*3*) and RNA amplification reaction (*4–6*) due to their high catalytic activity and fidelity (*7*). MMLV RT is a 75-kDa monomer, while AMV RT is a heterodimer consisting of 63-kDa α subunit and 95-kDa β subunit. MMLV RT comprises the fingers, palm, thumb, connection, and RNase H domains (*8–10*). This nomenclature, which was originally used in HIV-1 RT (*11*), is based on the resemblance to a right hand. The α subunit of AMV RT comprises these five domains, and the β subunit comprises these five domains and the C-terminal integrase domain (*12*).

RNA-dependent DNA polymerization (reverse transcription) and RNase H cleavage simultaneously occur when RT binds to a single template–primer (T/P). However, these two activities are thought to be functionally independent, based on the following evidences: (i) Each of MMLV RT and AMV RT exhibited the RNase H activity, but not the reverse transcription activity, when it binds to a T/P in the absence of dNTP (*13*); (ii) Crystal structural analysis of MMLV RT has revealed that the fingers, palm and thumb domains are involved in the reverse transcription activity while the RNase H domain is involved in the RNase H activity (*8–10*), and the RNase H domain (Ile498-Leu671) alone retains the RNase H activity (*10*); (iii) The mutations of the catalytically important residues in the fingers and palm domains [Arg110 (*14*) and Lys152 (*15*) of MMLV RT and Asp181 of AMV RT (*16*)] reduced or abolished the reverse transcription activity but did not affect the RNase H activity, while those in the RNase H domain [Asp524 and Asp583 of MMLV RT (*17*) and Asp505 of AMV RT (*16*)] abolished the RNase H activity but had no effect on the reverse transcription activity. In MMLV RT, crystal structure of the fingers, palm, thumb and connection domains (*9*) and that of the RNase H domain (*10*) have been independently determined, but that of the full length molecule has not. Therefore, these evidences have raised a structural model of MMLV RT that the RNase H domain is positioned far from the fingers/palm/thumb domain (*9*), like the p66 subunit of HIV-1 RT (*18*). However, the thermal stability of the reverse transcription activity of RT has been markedly improved by eliminating its RNase H activity (*19*). As a result, reaction temperature of MMLV RT and AMV RT for the reverse transcription has increased from 37–45°C to 50–60°C (*20*), suggesting that these two activities are not fully functionally independent.

In the previous report (*21*), we compared the thermal stabilities of the reverse transcription activity of MMLV RT and AMV RT, and showed that the intrinsic thermal

*To whom correspondence should be addressed. Tel: +81-75-753-6267, Fax: +81-75-753-6265,
E-mail: yasukawa@kais.kyoto-u.ac.jp

© The Authors 2008. Published by Oxford University Press on behalf of the Japanese Biochemical Society. All rights reserved.

Downloaded from http://jb.oxfordjournals.org/ at Islamic Azad University on September 28, 2012

stability of AMV RT is higher than that of MMLV RT and that AMV RT is stabilized by the T/P more potently than MMLV RT. In cDNA synthesis and RNA amplification, elevated reaction temperature has been highly desired because it reduces RNA secondary structure and non-specific binding of primer. The purpose of this study is to examine the role of each domain of MMLV RT and AMV RT on the differences in activity and stability between the two RTs. In other others, the purpose is to examine whether the differences in activity and stability between MMLV RT and AMV RT can be attributed to one of the five domains. We constructed and characterized four chimeric RTs (named MRT-AF, MRT-AP, MRT-AT and MRT-AR), which comprise one of the fingers, palm, thumb and RNase H domains originated from AMV RT, respectively, and the other three and connection domains originated from MMLV RT (Fig. 1). Unexpectedly, the reverse transcription activities, but not the RNase H activities, of all chimeric RTs were drastically reduced. Based on the results, we propose that there might be an interaction between the fingers/palm/thumb domain and the RNase H domain in MMLV RT, through which the reverse transcription and RNase H activities of MMLV RT are functionally coupled.

MATERIALS AND METHODS

Materials—Native AMV RT (Lot LS02207-7) purified from AMV was purchased from Life Sciences, Inc (Petersburg, FL). Poly(rA)•p(dT)$_{12–18}$ (Lot HA0166), dTTP (Lot 340755), [methyl-^{3}H]dTTP (1.52 TBq/mmol) (Lot 209), poly(rA) (Lot HI0066) and [methyl-^{3}H]poly(rA) (22 TBq/mmol) (Batch 32) were purchased from GE Healthcare (Buckinghamshire, UK). p(dT)$_{45}$ was purchased from Sigma-Aldrich Japan (Hokkaido, Japan). The glass filter GF/C 2.5 cm is a product of Whatman (Middlesex, UK). RT concentration was determined according to the method of Bradford (*22*) using Protein Assay CBB Solution (Nacalai Tesque, Kyoto, Japan) with bovine serum albumin (Lot M3G9751, Nacalai Tesque) as a standard. The expression plasmid for MMLV RT, pET-MRT, has been described previously (*21*).

Cloning of cDNA for the α Chain of AMV RT—RNA was prepared from the serum of chicken infected with AMV. cDNA for the *α* chain of AMV RT was amplified by RT–PCR with the primers AF1F and ARB (Table 1). The amplified DNA product was digested with the restriction enzymes *Nde*I and *Eco*RI and inserted in pET-22b(+) (Merck Bioscience, Tokyo, Japan) digested with *Nde*I and *Eco*RI to produce pET-ARTα. The nucleotide sequence of the cDNA for the *α* chain was determined by a Shimadzu DNA sequencer DSQ-2000 (Kyoto, Japan).

Construction of Chimeric MMLV/AMV RTs—The pET-MRT (*21*) and pET-ARTα were used as templates for PCR. The construction of chimeric MMLV/AMV RTs is illustrated in Fig. 1, in which F1, P1, F2, P2, T, C and R, represent the N-terminal portion of fingers, N-terminal portion of palm, C-terminal portion of fingers, C-terminal portion of palm, thumb, connection and RNase H domains, respectively. The primers used for PCR are listed in Table 1. The expression plasmid for MRT-AF, pET-MRT-AF, was constructed as follows. The 262-bp fragment (AF1) containing F1 of AMVRT, the 104-bp fragment (MP1) containing P1 of MMLV RT, the 146-bp fragment (AF2) containing F2 of AMV RT, and the 1,471-bp fragment (MP2R) containing P2, T, C and R of MMLV RT were amplified using the combinations of the primers AF1F and AF1B, MP1F and MP1B, AF2F and AF2B and MP2F and MRHISB, respectively. The 352-bp fragment (AF1MP1) containing F1 of AMV RT and P1 of MMLV RT was amplified from the mixture of AF1 and MP1 with the primers AF1F and MP1B. The 484-bp fragment

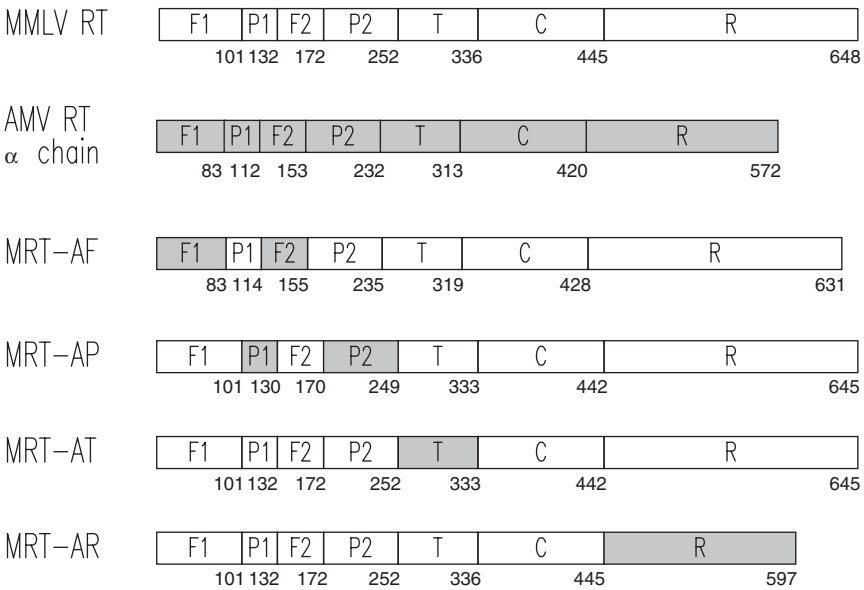

Fig. 1. **Construction of chimeric MMLV/AMV RTs.** The sequences of MMLV RT and the α chain of AMV RT are shown as open and filled bars, respectively. F1, P1, F2, P2, T, C and R indicate the N-terminal portion of fingers, N-terminal portion of palm, C-terminal portion of fingers, C-terminal portion of palm, thumb, connection and RNase H domains, respectively. The numbers represent the last amino acid of the respective region.

Downloaded from http://jb.oxfordjournals.org/ at Islamic Azad University on September 28, 2012

Table 1. **Primers.**

Primers	Sequences (5′–3′)
AF1F	TCCTGCAGCATATGACTGTTGCGCTACATCTGGCT
AF1B	GGAACAAGCTTAGCGTTAAC
MF1F	AAGGAGATATACATATGACATGGCTGTCTG
MF1B	TCTTCCACCCGCTTGTTGAC
AP1F	CAAGCGGGTGGAAGATTTTGGGGCCGTCCAACAGG
AP1B	AAGCAATCCTTGAGGTCT
MP1F	GCTAAGCTTGTTCCAATCCACCCCACCGTGCCCAA
MP1B	GCATCCTTTAAATCAAGCAC
AF2F	GATTTAAAGGATGCATTCTTTTCTATTCCTCTTGC
AF2B	GTGGGAGAACAGGTCATCCC
MF2F	AGACCTCAGGATTGCTTTTTCTGCCTGAGACTCC
MF2B	TGAGTTTTTGAAACC
AP2F	GGTTTCAAAAACTCACCCACTATCTGTCAGTTGAT
AP2B	TGAGCCTAACTTGTA
MP2F	GGGATGACCTGTTCTCCCACCCTGTTTGATGAGGC
MP2B	TCTTTTAGAAGATACCCCAG
ATF	TATCTTCTAAAAGAAACGTATGCAGCACCCGTAGG
ATB	TCGTTCCAAGGCAGC
MTF	TACAAGTTAGGCTCAGGTCAGAGATGGCTGACTGA
MCF	GCTGCCTTGGAACGACCAGATTTGACTAAGCCCTT
MCB	TAGAGTCCGRGRCCAAAAGCAAGGC
MRHISB	CTGAATTCTAGTGGTGATGGTGGTGGTGGAGGAGGGTAGAGGTGTCT
ARF	GCTTTTGGACAGGGACTCTATTTTTGACATTGCGC
ARB	CTGAATTCTTATTAATACGCTTGAAAGGTGGCTTG
ARHISB	CTGAATTCTAGTGGTGATGGTGGTGGTGATACGCTTGAAAGGTGG
D224A	TGCTACAGTACGTGGCTGACTTACTGCTGG
D224A_CP	CCAGCAGTAAGTCAGCCACGTACTGTAGCA
D524A	CACACCTGGTACACAGCTGGAAGCAGTCTC
D524A_CP	GAGACTGCTTCCAGCTGTGTACCAGGTGTG

(AF1MP1AF2) containing F1 of AMV RT, P1 of MMLV RT, and F2 of AMV RT was amplified from the mixture of AF1MP1 and AF2 with the primers AF1F and AF2B. Finally, the 1,935-bp fragment (AF1MP1AF2MP2R) containing F1 of AMV RT, P1 of MMLV RT, F2 of AMV RT and P2, T, C and R of MMLV RT was amplified from the mixture of AF1MP1AF2 and MP2R with the primers AF1F and MRHISB. The AF1MP1AF2MP2R was digested with the restriction enzymes *Nde*I and *Eco*RI and inserted in pET-22b(+) digested with *Nde*I and *Eco*RI to produce pET-MRT-AF. pET-MRT-AP was constructed using the primers MF1F, MF1B, AP1F, AP1B, MF2F, MF2B, AP2F, AP2B, MTF and MRHISB. pET-MRT-AT was constructed using the primers MF1F, MP2B, ATF, ATB, MCF and MRHISB. pET-MRT-AR was constructed using the primers MF1F, MCB, ARF and ARHISB. The expression plasmid for MRT-D224A (named pET-MRT-D224A), in which Asp224 is replaced with Ala, was constructed using the primers MF1F, D224A, D224A_CP and MRHISB, and that for MRT-D524A (named pET-MRT-D524A) was constructed using the primers MF1F, D524A, D524A_CP, and MRHISB. Their nucleotide sequences were verified by the DNA sequencer DSQ-2000. *Escherichia coli* BL21(DE3) [F^-, *ompT*, *hsdS*$_B$ (r_B^- m_B^-) *gal dcm* (DE3)] cells were transformed with each of the resulted plasmids.

Expression and Purification of RTs—Three mililitres of L broth containing 50 μg ml^{-1} ampicillin was inoculated with the glycerol stock of the transformed BL21(DE3) and incubated for 16 h with shaking at 30°C. The expression of the RT gene was induced by the auto-induction system (Novagen, Darmstadt, Germany). The cells were harvested by centrifugation at 10,000 × *g* for 10 min and disrupted by FastBreak Cell Lysis Reagent (Promega, Madison, WI). The suspension was mixed with 50 μl of HisLink Protein Purification Resin (Promega). The bound RT was eluted with 1 ml of 100 mM HEPES–NaOH (pH 7.5), 10 mM imidazole. Solid $(NH_4)_2SO_4$ was added to the eluate to be 20% saturation. The pellet resulted was collected by centrifugation at 15,000 × *g* for 20 min and dissolved in 0.1 ml of 100 mM HEPES–NaOH (pH 7.5), 10 mM imidazole.

SDS–PAGE—SDS–PAGE was performed in a 10% polyacrylamide gel under reducing conditions according to the method of Laemmli (*23*). Proteins were reduced by treatment with 2.5% of 2-mercaptoethanol at 100°C for 10 min, and then applied onto the gel. A constant current of 40 mA was applied for 40 min. After electrophoresis, proteins were stained with Coomassie Brilliant Blue R-250. The molecular mass marker kit consisting of myosin (200 kDa), β-galactosidase (116 kDa), bovine serum albumin (66.3 kDa), rabbit muscle aldolase (42.4 kDa), and bovine erythrocyte carbonic anhydrase (30.0 kDa) was a product of Daiichi Pure Chemicals (Tokyo, Japan).

Reverse Transcription Assay—Reverse transcription activity was determined by measuring the incorporation of [^{3}H]dTTP to poly(rA)•p(dT)$_{12-18}$. The reaction was

Downloaded from http://jb.oxfordjournals.org/ at Islamic Azad University on September 28, 2012

carried out in 25 mM Tris–HCl (pH 8.3), 50 mM KCl, 2 mM DTT, 5 mM $MgCl_2$, 25 μM poly(rA)•p$(dT)_{12-18}$ (the concentration is expressed as that of p$(dT)_{12-18}$), 0.4 mM [^{3}H]dTTP (3.7 MBq/ml, 1.85 Bq/pmol) and RT (5 nM for AMV RT and MMLV RT and 860–1,500 nM for chimeric RTs) at 37°C. Aliquot (20 μl) was taken from the reaction mixture at specified time and immediately spotted onto the glass filter. Unincorporated [^{3}H]dTTP was removed by three washes of chilled 5%(w/v) trichloroacetic acid (TCA) for 10 min each followed by one wash of chilled 95% ethanol. The radioactivity of the dried filters was counted in 2.5 ml of Opti-Fluor (PerkinElmer, Waltham, MA). The initial reaction rate was estimated by the time-course of the amounts of [^{3}H]dTTP incorporated. The kinetic parameters, k_{cat} and K_m, were determined based on the Michaelis–Menten equation using the non-linear least-squares methods (*24*) with Kaleida Graph Version 3.5 (Synergy Software, Essex, VT).

RNase H Assay—RNase H activity was determined by measuring the [^{3}H]oligo(rA) released from [^{3}H]poly(rA)•p$(dT)_{45}$. The reaction was carried out in 25 mM Tris–HCl (pH 8.3), 50 mM KCl, 2 mM DTT, 5 mM $MgCl_2$, 25 μM [^{3}H]poly(rA)•p$(dT)_{45}$ (the concentration is expressed as that of the total nucleotide) (22 kBq/ml, 2.2 Bq/pmol), 0.003%(w/v) bovine serum albumin, and RT (10 nM for AMV RT, 100 nM for MMLV RT, and 220 or 290 nM for chimeric RTs) at 37°C. At specified time, the reaction mixture (50 μl) was placed on ice and mixed with 20 μl of 50 mM EDTA, 0.1 M sodium pyrophosphate, 28 μl of 1.0 mg/ml sheared DNA from calf thymus, and 32 μl of chilled 40%(w/v) TCA. After 10 min, the solution was centrifuged at $9,000 \times g$ at 4°C for 10 min. The radioactivity of the supernatant (65 μl) was counted in 2.5 ml of Opti-Fluor. The initial reaction rate was estimated by the time-course of the amounts of 10%(w/v) TCA-soluble RNA.

RESULTS

Cloning of the α Chain of AMV RT—We prepared the RNA from the AMV-containing chicken serum and amplified the cDNA for the AMV RT α chain by RT–PCR with the primers AF1F and ARB (Table 1), which was designed based on the nucleotide sequence of avian leucosis virus RT gene (GenBank accession code M37980). The cloned cDNA contained 1,716 bp and encodes 572 amino-acid residues. Sequences have been deposited with GenBank under accession code FJ041197. Sequence comparison revealed that the nucleotide sequence of the cDNA for the AMV RT α chain differed at 23 (T148, T204, G276, C300, C315, A656, C693, C704, T810, T877, A911, C1045, C1114, G1185, G1200, G1236, A1326, C1347, A1431, C1458, A1554, T1584 and G1682) from that of M37980, but the deduced amino-acid sequence differed only at 4 (Lys219, Gln304, Glu395 and Gly561). To test that the cDNA we cloned encodes the active RT, we constructed the recombinant vaculovirus vector harbouring this cDNA, and transfected it into the insect cells. The reverse transcription activity was detected in the soluble fraction of the transfected cells (data not shown), showing that this cDNA encodes the active enzyme.

Construction of Chimeric RT—Figure 2 shows the comparison of the amino-acid sequences between MMLV RT (J02255) and AMV RT (FJ041197). Both enzymes have all the fingers, palm, thumb, connection and RNase H domains. Each of the fingers and palm domains are further divided into the N- and C-terminal portions. It has been reported that recombinant MMLV RT has been expressed in soluble fractions in *E. coli*, from which sufficient amounts of active enzymes have been purified (*21*, *25–27*), whereas recombinant AMV RT has hardly been expressed in soluble fractions in *E. coli* (*28*). We therefore designed four MMLV/AMV chimeric RTs (named MRT-AF, MRT-AP, MRT-AT and MRT-AR) which comprise one of the fingers, palm, thumb and RNase H domains originated from AMV RT, respectively, and the other three and connection domains originated from MMLV RT (Fig. 1). We also designed two MMLV RT variants (named MRT-D224A and MRT-D524A) as a negative control, in which the catalytically important residue for the reverse transcription activity, Asp224 and that for the RNase H activity, Asp524, were substituted with Ala, respectively.

MMLV RT and the four chimeric RTs were expressed in *E. coli* and purified as described in the section of MATERIALS AND METHODS section. Upon SDS–PAGE under a reducing condition, MMLV RT yielded a single band with a molecular mass of 75 kDa, and AMV RT, which was purified from AMV, yielded two bands with molecular masses of 95 and 63 kDa (Fig. 3). MRT-AF, MRT-AP, MRT-AT, and MRT-AR yielded major single bands with molecular masses in the range of 65–73 kDa, each corresponding to their calculated molecular masses (70,203, 71,342, 71,973 and 66,387 Da, respectively). MRT-D224A and MRT-D524A yielded a single band with a molecular mass of 75 kDa (data not shown).

Specific Activities of Chimeric RTs—We measured the reverse transcription and RNase H activities of MMLV RT, AMV RT and the four chimeric RTs. The specific activities are summarized in Table 2. MMLV RT exhibited higher specific reverse transcription activity and lower specific RNase H activity than AMV RT, which are coincident with the previous reports (*21*, *25–27*, *29*). The specific activities of the chimeric RTs for the reverse transcription reaction were 0.005–0.09% of that of MMLV RT, while those for the RNase H reaction were 19–25% of that of MMLV RT, indicating that in all chimeric RTs, the reverse transcription activities were markedly reduced but the RNase H activities were substantially retained. MRT-D224A completely lost the reverse transcription activity, and MRT-D524A completely lost the RNase H activity, indicating that the contamination of *E. coli* enzymes, such as RNase HI and HII, in the enzyme preparations could be negligible if any. The RNase H activity of MRT-D224A and the reverse transcription activity of MRT-D524A were comparable to those of MMLV RT.

To study the steady-state kinetic parameters that contribute to the marked decrease in the specific reverse transcription activities of the chimeric RTs, we measured the initial reaction rates for the reverse transcription activity at various dTTP concentrations (0–400 μM) with MRT-AF (860 nM) at 37°C (Fig. 4). A saturated profile of

Downloaded from http://jb.oxfordjournals.org/ at Islamic Azad University on September 28, 2012

Fig. 2. **A sequence alignment of MMLV RT and AMV RT.** Homology search was performed using the search program DDBJ CLUSTALW and revised based on the data of X-ray crystallographic analysis of MMLV RT (*8-10*). F1, P1, F2, P2, T, C and R correspond to those in Fig. 1. M and A indicate MMLV RT and AMV RT, respectively. Amino-acid numberings of MMLV RT and AMV RT are according to GenBank accession codes J02255 and FJ041197, respectively. Asterisks show homologous amino-acid residues. The overall sequence homology is 23%. The sequence homology of F1, P1, F2, P2, T, C, and R are 22%, 35%, 28%, 35%, 21%, 26% and 17%, respectively. The polypeptide region Pro480-Arg506 of MMLV RT is underlined.

the Michaelis–Menten kinetics was obtained, and the K_m and k_{cat} values were separately determined (Table 3), suggesting that the decrease in the specific reverse transcription activity of MRT-AF can be ascribed to the decrease in k_{cat}. The initial reaction rates of the other three chimeric RTs at low dTTP concentrations (0–100 μM) could not be obtained due to poor activities (data not shown). However, based on the specific activities obtained by the reaction with the dTTP concentration of 400 μM (Table 2), their k_{cat} values were thought to be lower than that of MRT-AF [$(0.013 \pm 0.001)\,s^{-1}$].

We next measured the initial reaction rates for the RNase H reaction at various poly(rA)•p(dT)$_{45}$ concentrations (0–25 μM in total nucleotide) with MMLV RT (100 nM), AMV RT (10 nM) and the four chimeric RTs (220 nM), at 37°C (Fig. 5). For chimeric RTs, a saturated profile of the Michaelis–Menten kinetics was obtained, and the K_m and k_{cat} values were separately determined (Table 3). For MMLV RT and AMV RT, the initial reaction rates increased linearly with increasing poly(rA)•p(dT)$_{45}$ concentration, and their K_m and k_{cat} values were thought to be substantially higher than those of the chimeric RTs. Therefore, the decrease in the activity of the chimeric RTs can be ascribed to the decrease in k_{cat} value. It was previously reported that the K_m, k_{cat}, and k_{cat}/K_m values in the RNase H reaction at 37°C of HIV-1 RT were 5.4 μM, $0.054\,s^{-1}$, and $10{,}000\,M^{-1}s^{-1}$, respectively, and those of HIV-2 RT were 49.9 μM, $0.041\,s^{-1}$ and $800\,M^{-1}s^{-1}$, respectively (*30*). Therefore, it might be said that the k_{cat}/K_m values of MMLV RT and AMV RT in the RNase H reaction are significantly lower than that of HIV-1 RT but comparable to that of HIV-2 RT.

Downloaded from http://jb.oxfordjournals.org/ at Islamic Azad University on September 28, 2012

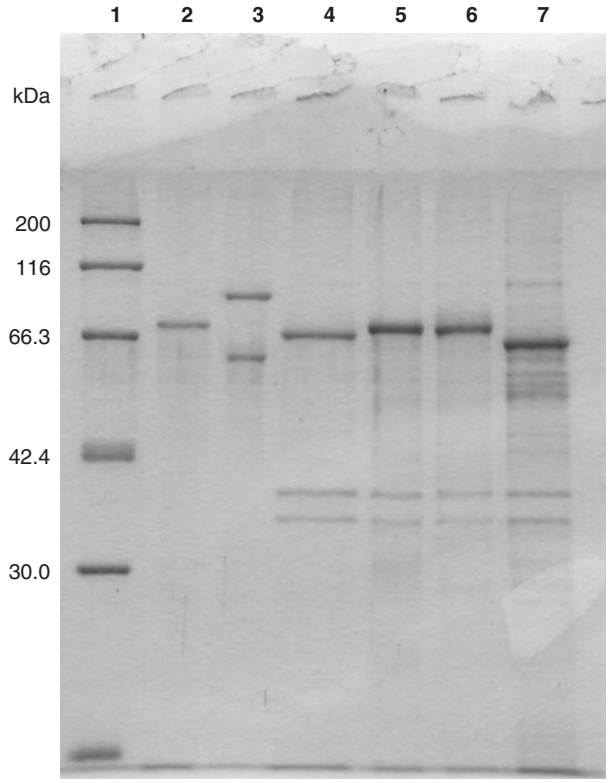

Fig. 3. **SDS–PAGE of RT under reducing condition.** Lane 1, molecular-mass marker; lane 2, MMLV RT (0.5 μg); lane 3, AMV RT (0.7 μg); lane 4, MRT-AF (1.6 μg); lane 5, MRT-AP (1.2 μg); lane 6, MRT-AT (1.1 μg), lane 7, MRT-AR (1.6 μg).

Table 2. **Specific activity of RT at 37°C.**

	Reverse transcription (units/mg)[a]	RNase H (units/mg)[b]
MMLV RT	130,000 ± 70,000 (1.0)	53,000 ± 2,000 (1.0)
AMV RT	32,000 ± 6,000 (0.25)	192,000 ± 6,000 (3.6)
MRT-AF	120 ± 50 (9×10^{-4})	10,000 ± 4,000 (0.19)
MRT-AP	90 ± 49 (7×10^{-4})	10,000 ± 5,000 (0.19)
MRT-AT	6 ± 3 (5×10^{-5})	13,000 ± 6,000 (0.25)
MRT-AR	15 ± 8 (1×10^{-4})	11,000 ± 6,000 (0.21)
MRT-D224A	ND[c]	42,000 ± 10,000 (0.79)
MRT-D524A	134,000 ± 32,000 (1.0)	ND[c]

The average of triplicate determination with SD values is shown. Numbers in parentheses indicate the values relative to MMLV RT. Molecular masses used for the calculation are 72,161, 153,110, 70,203, 71,342, 71,973, 66,387, 72,117 and 72,117 Da for MMLV RT, AMV RT, MRT-AF, MRT-AP, MRT-AT, MRT-AR, MRT-D224A and MRT-D524A, respectively. [a]The reaction was carried out in 25 mM Tris–HCl (pH 8.3), 50 mM KCl, 2 mM DTT, 5 mM $MgCl_2$, 25 μM poly(rA)•p(dT)$_{12–18}$ (the concentration is expressed as that of p(dT)$_{12–18}$) and 0.4 mM [^{3}H]dTTP at 37°C. One unit is defined as the amount which incorporates 1 nmol of dTTP into poly(rA)•p(dT)$_{12–18}$ in 10 min. [b]The reaction was carried out in 25 mM Tris–HCl (pH 8.3), 50 mM KCl, 2 mM DTT, 5 mM $MgCl_2$ and 25 μM [^{3}H]poly(rA)•p(dT)$_{45}$ (the concentration is expressed as that of the total nucleotide), and 0.003%(w/v) bovine serum albumin at 37°C. One unit is defined as the amount which makes 1 pmol oligo(rA) (the amount is expressed as that of the total nucleotide) of 10%(w/v) TCA-soluble RNA in 20 min. [c]ND, not detectable.

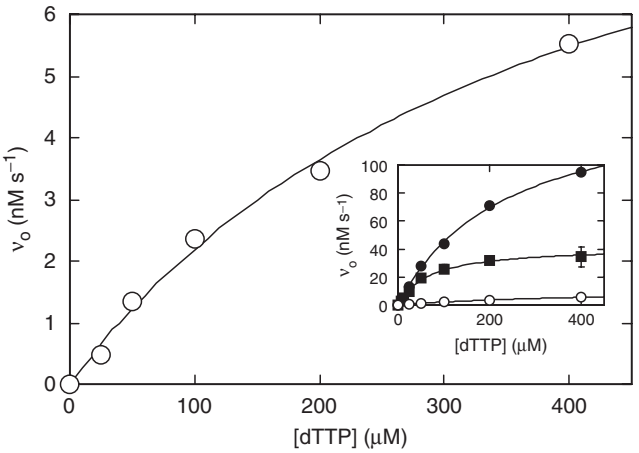

Fig. 4. **Dependence on the substrate concentration of the initial reaction rate of RT-catalysed reverse transcription**. The reaction was carried out with MRT-AF (open circle) at 860 nM, at 37°C. Inset shows MRT-AF (open circle) at 860 nM, MMLV RT (closed circle) at 5 nM, and AMV RT (closed square) at 5 nM, at 37°C. The concentration of poly(rA)•p(dT)$_{12–18}$ was 25 μM. Error bars indicate SD values. Solid line represents the best fit of the Michaelis–Menten equation with the non-linear least-squares methods.

Table 3. **Kinetic parameters of RT at 37°C.**

	K_m (μM)	k_{cat} (s^{-1})	k_{cat}/K_m ($M^{-1} s^{-1}$)
	Reverse transcription reaction		
MMLV RT[a]	232 ± 19	33 ± 1	140,000 ± 10,000
AMV RT[a]	67.2 ± 8.5	8.3 ± 0.4	120,000 ± 10,000
MRT-AF	402 ± 78	0.013 ± 0.001	32 ± 3
	RNase H reaction		
MMLV RT	> 25	> 3.0×10^{-3}	130 ± 3
AMV RT	> 25	> 2.5×10^{-2}	1000 ± 14
MRT-AF	13 ± 3	(6.3 ± 0.8) × 10^{-4}	49 ± 7
MRT-AP	7.0 ± 2.2	(3.8 ± 0.5) × 10^{-4}	54 ± 11
MRT-AT	8.9 ± 1.7	(4.6 ± 0.4) × 10^{-4}	51 ± 6
MRT-AR	4.3 ± 1.3	(2.4 ± 0.3) × 10^{-4}	57 ± 13

The average of triplicate determination with SD value is shown. [a]Ref. 21.

Optimal Reaction Temperature of RT in the RNase H Reaction—It was reported that thermal stability of the reverse transcription activity of RT has been markedly improved by eliminating its RNase H activity (*19*). Therefore, it was of interest to study the optimal reaction temperature of the chimeric RTs in the RNase H reaction. Figure 6 shows the RNase H activities of MMLV RT, AMV RT and the chimeric RTs at various temperatures ranging 30–60°C. MMLV RT and AMV RT showed a curve with the optimal temperature range of around 44–50°C. The optimal reaction temperatures of the chimeric RTs were in the range of 48–52°C, being higher by 2–4°C than those of MMLV RT and AMV RT. The relative activities at 52–60°C of the chimeric RTs were higher than those of MMLV RT and AMV RT, and those at 30–40°C of the chimeric RTs was lower than that of MMLV RT but almost the same as that of AMV RT. These results showed that all chimeric RTs are more

Downloaded from http://jb.oxfordjournals.org/ at Islamic Azad University on September 28, 2012

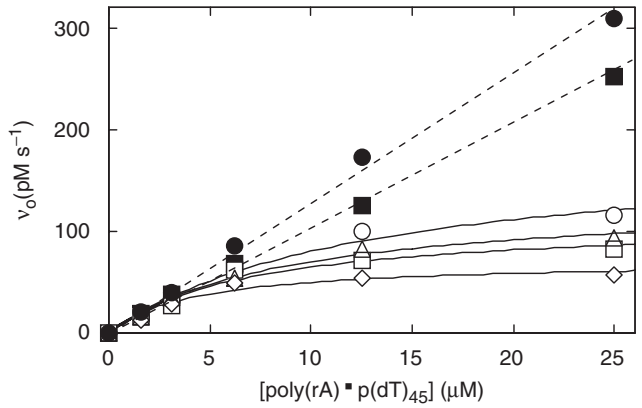

Fig. 5. **Dependence on the substrate concentration of the initial reaction rate of RT-catalysed RNase H reaction**. The reaction was carried out with MMLV RT (closed circle) at 100 nM, AMV RT (closed square) at 10 nM, MRT-AF (open circle) at 290 nM, MRT-AP (open square) at 290 nM, MRT-AT (open triangle) at 290 nM, and MRT-AR (open diamond) at 290 nM, at 37°C. Solid line represents the best fit of the Michaelis–Menten equation with the non-linear least-squares methods, and broken line represents the best fit using the linear function with the linear least-squares methods.

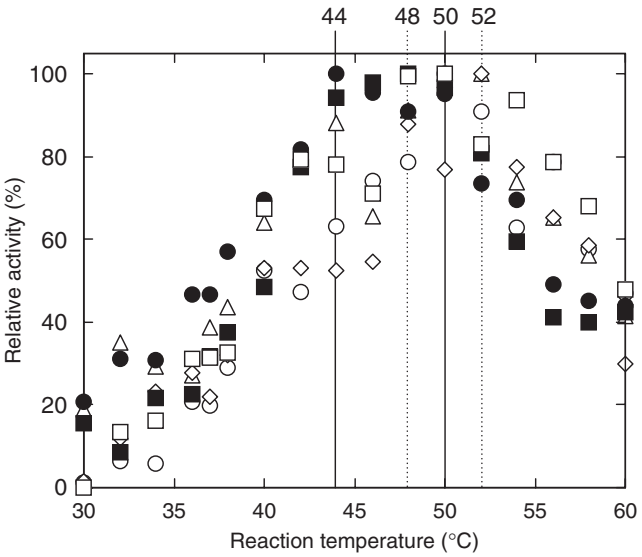

Fig. 6. **Dependence on temperature of the initial reaction rate of RT-catalysed RNase H reaction**. The reaction was carried out with MMLV RT (closed circle) at 50 nM, AMV RT (closed square) at 5 nM, MRT-AF (open circle) at 220 nM, MRT-AP (open square) at 220 nM, MRT-AT (open triangle) at 220 nM, and MRT-AR (open diamond) at 220 nM. The relative activity is defined as the ratio of the initial reaction rate at the indicated temperature to that at the optimal temperature (272 pM s^{-1} at 44°C for MMLV RT; 315 pM s^{-1} at 48°C for AMV RT; 332 pM s^{-1} at 50°C for MRT-AF; 277 pM s^{-1} at 54°C for MRT-AP; 338 pM s^{-1} at 52°C for MRT-AT; and 319 pM s^{-1} at 52°C for MRT-AR). The optima (middle of the temperature range at which the relative activity was > 80%) are indicated by solid vertical lines for MMLV RT and AMV RT and by broken vertical lines for MRT-AF, MRT-AP, MRT-AT and MRT-AR.

thermally stable than MMLV RT and AMV RT in the RNase H reaction.

DISCUSSION

Interaction of the Fingers/Palm/Thumb Domain and the RNase H Domain in MMLV RT—All chimeric MMLV/AMV RTs almost lacked the reverse transcription activity, but retained the RNase H activity (Table 2). Therefore, the differences in the activity and stability between MMLV RT and AMV RT could not be attributed to one of the five domains. The active sites for the reverse transcription reaction in MRT-AF, MRT-AP and MRT-AT were impaired by exchanging the fingers, palm and thumb domains of MMLV RT, respectively, with the corresponding domains of AMV RT domains. This is comprehensible because the fingers/palm/thumb domain is involved in the reverse transcription activity. However, the active site for the reverse transcription activity of MRT-AR was impaired by exchanging the RNase H domain of MMLV RT with that of AMV RT. This is easily comprehensible by hypothesizing the interaction between the active site for the reverse transcription reaction and that for the RNase H reaction. We therefore propose that there might be an interaction between the fingers/palm/thumb domain and the RNase H domain in MMLV RT, and that this interaction affects the reverse transcription activity rather than the RNase H activity. However, it should be mentioned that the reverse transcription activity of MRT-AR was impaired by the structural change associated with the substitution of the RNase H domain of MMLV RT with that of AMV RT cannot be ruled out from the results presented in this study.

Insights into the Whole Structure of MMLV RT—In MMLV RT, crystal structure of the fingers, palm, thumb and connection domains (Thr24-Pro474) (*9*) and that of the RNase H domain (His503-Ser668) (*10*) have been independently determined. The former was determined from the crystal of the full length MMLV RT (Thr24-Leu671). This means that crystal structure of the RNase H domain was not determined from the crystal of the full length MMLV RT (*9*). The structure of the RNase H domain was determined from the crystal of the isolated RNase H domain of MMLV RT (Ile498-Leu671) (*10*). Therefore, crystal structure of the full length molecule has not been determined yet. Das *et al*. (*9*) and Cote *et al*. (*32*) proposed the structural model of MMLV RT that the RNase H domain is positioned far from the fingers/palm/thumb domain (Fig. 7A), based on the structure of the p66 subunit in the crystal of HIV-1 RT (*18*). In HIV-1 RT, the p66 subunit has all five domains while the p51 subunit lacks the RNase H domain, and the reverse transcription and RNase H activities reside only in p66. Importantly, the polypeptide region Asp113-Pro140 in the fingers domain of p51 interacts with the palm domain of p66, supporting the floor of the reverse transcription active site of p66 (*33*, *34*).

Interestingly, Pandey *et al*. reported that the insertion of the 27 amino-acid peptide corresponding to Pro480-Arg506 in the RNase H domain of MMLV RT (Fig. 2) into

Downloaded from http://jb.oxfordjournals.org/ at Islamic Azad University on September 28, 2012

the connection domain of p66 of HIV-1 RT resulted in a monomeric p66 which lacked the reverse transcription activity but possessed the RNase H activity (*35*). They pointed out that there is 21% (7 out of 34) sequence homology between the Pro480-Arg506 of MMLV RT and the Asp113-Pro140 of HIV-1 RT, proposing a model that in the monomeric p66, the inserted Pro480-Arg506 interacts with the palm domain of the same molecule, as does the Asp113-Pro140 of p51 with the palm domain of p66 in the heterodimeric HIV-1 RT (*35*, *36*). AMV RT does not have such sequence according to the sequence comparison (Fig. 2). Considering the results by Pandey *et al* (*35*, *36*) and that the crystal structure of Val475-Ala502 in MMLV RT has not been determined, we propose a new structural model for MMLV RT (Fig. 7B). In this model, the polypeptide region Pro480-Arg506 of the RNase H domain interacts with the fingers/palm/thumb domain, supporting the floor of the reverse transcription active-site cleft of MMLV RT, as the polypeptide region Asp113-Pro140 of p51 interacts with the palm domain of p66 in the heterodimeric HIV-1 RT. Through this interaction, the reverse transcription and RNase H activities of MMLV RT are thought to be functionally coupled. This inter-molecular interaction resembles that of a genetically engineered fusion protein of a cytokine and its receptor (*37*).

Increase in Thermal Stabilities of the RNase H Activities of the Chimeric RTs—It is well known that there is a compromise between activity and stability in various enzymes (*38–41*). This is understood by that local instability should be required for substrate binding and catalysis. However, in our study with thermolysin (a thermostable neutral zinc metalloproteinase), the thermal stability of thermolysin is governed by a local unfolding far from the active site, and thus there is no such compromise (*42*, *43*).

In this study, we showed that the RNase H activity of RT increased by reducing its reverse transcription activity although the degree of the increase was small. The thermal stabilities of MMLV RT and AMV RT in the reverse transcription activity substantially increase by eliminating the RNase H activity (*19*, *20*). One possibility is that the thermal stability of MMLV RT is governed by the region Pro480-Arg506, and that the instability of this region should be required for the RNase H activity, but not the reverse transcription activity.

Difference between MMLV RT and AMV RT—There are several differences in activity, stability, solubility and structure between MMLV RT and AMV RT: (i) MMLV RT is more active than AMV RT in the reverse transcription reaction, while AMV RT is more active than MMLV RT in the RNase H reaction (Table 2); (ii) The intrinsic thermal stability of AMV RT is higher than that of MMLV RT, and AMV RT is stabilized by the T/P more potently than MMLV RT (*21*, *31*); (iii) Recombinant MMLV RT has been expressed in the soluble fraction of *E. coli* (*21*, *25–27*), but recombinant AMV RT has hardly been expressed (*25–28*); (iv) MMLV RT is a monomer while AMV RT is a heterodimer. Because HIV-1 RT is a dimmer, AMV RT is thought to be more similar to HIV-1 RT than MMLV RT. However, our results suggest that

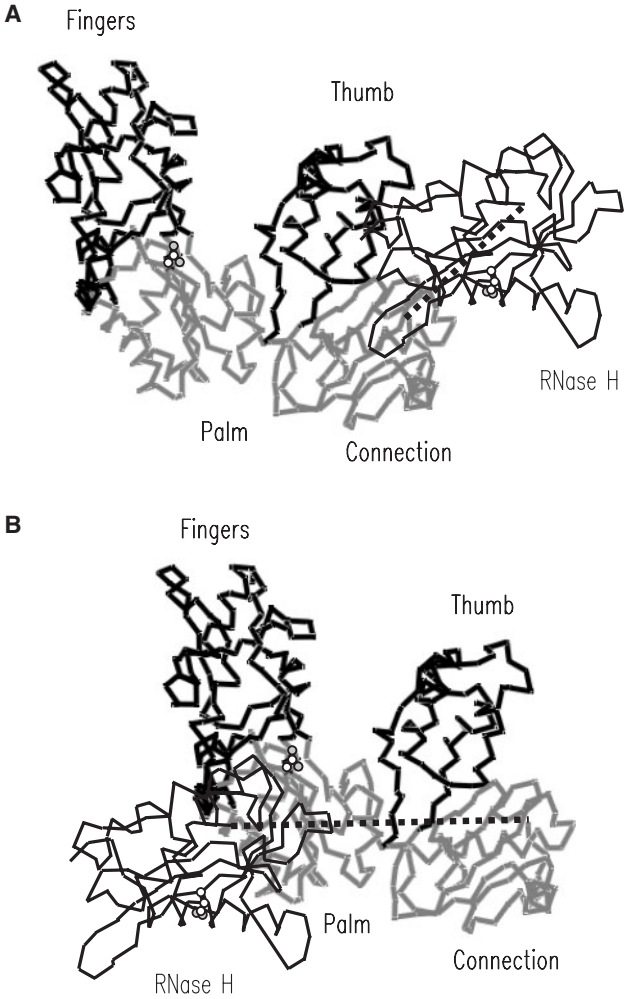

Fig. 7. **Proposed overall structure of MMLV RT.** (A) Model structure by Das *et al*. (*9*). (B) Model structure proposed in this study. The models were built by the combination of the two independent crystal structures, one for the polypeptide region Thr24-Pro474 corresponding to the fingers, palm, thumb and connection domains and the first six amino-acid residues of the RNase H domain (PDB accession code 1RW3) and the other for the polypeptide region His504-Ser668 corresponding to the RNase H domain (2HB5), based on the assumption that the RNase H domain is positioned far from the fingers/palm/thumb domain (A) and that the RNase H domain interacts with the fingers/palm/thumb domain (B). The dotted line connects Pro474 and His504. The side chain of Asp224 and Asp524, which are the catalytically important residues in the palm and RNase H regions, respectively, are shown. Atoms: carbon, white; oxygen, grey.

MMLV RT might be more similar to HIV-1 RT than AMV RT in respect of the domain–domain interaction. In support of this, both MMLV-RT (*21*, *25–27*) and HIV-1 RT (*44*) has been expressed in *E. coli* while AMV RT has not (*25–28*).

This study undertaken here was initially aimed toward exploring the role of each domain of MMLV RT and AMV RT on the differences in activity and stability between the two RTs. However, the results suggested a possibility for the interaction between the fingers/palm/thumb

Downloaded from http://jb.oxfordjournals.org/ at Islamic Azad University on September 28, 2012

domain and the RNase H domain in MMLV RT. Further study of this domain–domain interaction will lead to understanding the similarity and differences between RTs and generation of genetically engineered RT with high activity and stability.

ACKNOWLEDGEMENTS

We appreciate Dr Susumu Ueda, the chairman of Nippon Institute for Biological Science for kindly giving us the chicken serum containing AMV.

FUNDING

This study was supported in part (to K.Y.) by Grants-in-Aid for Scientific Research (No. 19580104) from the Japan Society of the Promotion of Sciences.

CONFLICT OF INTEREST

None declared.

REFERENCES

1. Temin, H.M. and Mizutani, S. (1970) RNA-dependent DNA polymerase in virions of Rous sarcoma virus. *Nature* **226**, 1211–1213
2. Baltimore, D. (1970) RNA-dependent DNA polymerase in virions of RNA tumour viruses. *Nature* **226**, 1209–1211
3. Kimmel, A.R. and Berger, S.L. (1987) Preparation of cDNA and the generation of cDNA libraries: overview. *Methods Enz.* **152**, 307–16
4. Kievits, T., van Gemen, B., van Strijp, D., Schkkink, P., Dircks, M., Adriaanse, H., Malek, L., Sooknanan, R., and Lens, P. (1991) NASBA isothermal enzymatic in vitro nucleic acid amplification optimized for the diagnosis of HIV-1 infection. *J. Virol. Methods* **35**, 273–286
5. Ishiguro, T., Saitoh, J., Horie, R., Hayashi, T., Ishizuka, T., Tsuchiya, S., Yasukawa, K., Kido, T., Nakaguchi, Y., Nishibuchi, M., and Ueda, K. (2003) Intercalation activating fluorescence DNA probe and its application to homogeneous quantification of a target sequence by isothermal sequence amplification in a closed vessel. *Anal. Biochem.* **314**, 77–86
6. Masuda, N., Yasukawa, K., Isawa, Y., Horie, R., Saito, J., Ishiguro, T., Nakaguchi, Y., Nishibuchi, M., and Hayashi, T. (2004) Rapid detection of *tdh* and *trh* mRNAs of *Vibrio parahaemolyticus* by the transcription-reverse transcription concerted (TRC) method. *J. Biosci. Bioeng.* **98**, 236–243
7. Roberts, J.D., Bebenek, K., and Kunkel, T.A. (1988) The accuracy of reverse transcriptase from HIV-1. *Science* **242**, 1171–1173
8. Georgiadis, M.M., Jessen, S.M., Ogata, C.M., Telesnitsky, A., Goff, S.P., and Hendrickson, W.A. (1995) Mechanistic implications from the structure of a catalytic fragment of Moloney murine leukemia virus reverse transcriptase. *Structure* **3**, 879–892
9. Das, D. and Georgiadis, M.M. (2004) The crystal structure of the monomeric reverse transcriptase from Moloney murine leukemia virus. *Structure* **12**, 819–829
10. Lim, D., Gregorio, G.G., Bingman, C., Martinez-Hackert, E., Hendrickson, W.A., and Goff, S.P. (2006) Crystal structure of the Moloney murine leukemia virus RNaseH domain. *J. Virol.* **80**, 8379–8389
11. Khlstaedt, L.A., Wang, J., Friedman, J.M., Rice, P.A., and Steitz, T.A. (1992) Crystal structure at 3.5 Å resolution of HIV-1 reverse transcriptase complexed with an inhibitor. *Science* **256**, 1783–1790
12. Bieth, E. and Darlix, J.-L. (1991) Complete nucleotide sequence of a highly infectious avian leucosis virus. *Nucleic Acids Res.* **20**, 367
13. DeStefano, J.J., Buiser, R.G., Mallaber, L.M., Myers, T.W., Bambara, R.A., and Fay, P.J. (1991) Polymerization and RNase H activities of reverse transcriptases from Avian myeloblastosis, human immunodeficiency, and Moloney murine leukemia viruses are functionally uncoupled. *J. Biol. Chem.* **266**, 7423–7431
14. Chowdhury, K., Kaushik, N., Pandey, V.N., and Modak, M.J. (1996) Elucidation of the role of Arg110 of murine leukemia virus reverse transcriptase in the catalytic mechanism: biochemical characterization of its mutant enzymes. *Biochemistry* **35**, 16610–16620
15. Shi, Q., Singh, K., Srivastaba, A., Kaushik, N., and Modak, M.J. (2002) Lysine 152 of MuLV reverse transcriptase is required for the integrity of the active site. *Biochemistry* **41**, 14831–14842
16. Werner, S. and Wohrl, B.M. (2000) Asymmetric subunit organization of heterodimeric Rous sarcoma virus reverse transcriptase αβ: localization of the polymerase and RNase H active sites in the α subunit. *J. Virol.* **74**, 4740–4744
17. Goedken, E.R. and Marqusee, S. (1999) Metal binding and activation of the ribonuclease H domain from Moloney murine leukemia virus. *Protein Eng.* **12**, 975–980
18. Huang, H., Chopra, R., Verdine, G.L., and Harrison, S.C. (1998) Structure of covalently trapped catalytic complex of HIV-1 reverse transcriptase: implications for drug resistance. *Science* **282**, 1669–1675
19. Kotewicz, M.L., Sampson, C.M., D'Alessio, J.M., and Gerard, G.F. (1988) Isolation of cloned Moloney murine leukemia virus reverse transcriptase lacking ribonuclease H activity. *Nucleic Acids Res.* **16**, 265–277
20. Gerard, G.F., Schmidt, B.J., Kotewicz, M.L., and Campbell, J.H. (1992) cDNA synthesis by Moloney murine leukemia virus RNase H-minus reverse transcriptase possessing full DNA polymerase activity. *Focus* **14**, 91–93
21. Yasukawa, K., Nemoto, D., and Inouye, K. (2008) Comparison of the thermal stabilities of reverse transcriptases from avian myeloblastosis virus and Moloney murine leukaemia virus. *J. Biochem.* **143**, 261–268
22. Bradford, M.M. (1976) A rapid and sensitive method for the quantitation of microgram quantities of protein utilizing the principle of protein-dye binding. *Anal. Biochem.* **72**, 248–254
23. Laemmli, U.K. (1970) Cleavage of structural proteins during the assembly of the head of bacteriophage T4. *Nature* **227**, 680–685
24. Sakoda, M. and Hiromi, K. (1976) Determination of the best-fit values of kinetic parameters of the Michaelis-Menten equation by the method of least squares with Taylor expansion. *J. Biochem.* **80**, 547–555
25. Kotewicz, M.L., D'Alessio, J.M., Driftmier, K.M., Blodgett, K.P., and Gerard, G.F. (1985) Cloning and over-expression of Moloney murine leukemia virus reverse transcriptase in *Escherichia coli*. *Gene* **35**, 249–258
26. Tanese, N., Roth, M., and Goff, S.P. (1985) Expression of enzymatically active reverse transcriptase in *Escherichia coli*. *Proc. Natl Acad. Sci. USA* **82**, 4944–4948
27. Roth, M.J., Tanese, N., and Goff, S.P. (1985) Purification and characterization of murine retroviral reverse transcriptase expressed in *Escherichia coli*. *J. Biol. Chem.* **260**, 9326–9335
28. Soltis, D.A. and Skalka, A.M. (1988) The α and β chains of avian retrovirus reverse transcriptase independently expressed in *Escherichia coli*: characterization of enzymatic activities. *Proc. Natl Acad. Sci. USA* **85**, 3372–3376
29. Werner, S. and Wohrl, B.M. (1999) Soluble Rous sarcoma virus reverse transcriptases a, ab, and b purified from insect cells are processive DNA polymerases that lack an RNase H

Downloaded from http://jb.oxfordjournals.org/ at Islamic Azad University on September 28, 2012

3'→5' directed processing activity. *J. Biol. Chem.* **374**, 26329–26336
30. Sevilya, Z., Loya, S., Adir, N., and Hizi, A. (2003) The ribonuclease H activity of the reverse transcritpases of human immunodeficiency viruses type 1 and type 2 is modulated by residue 294 of the small subunit. *Nucleic Acids Res.* **31**, 1481–1487
31. Gerard, G.F., Potter, R.J., Smith, M.D., Rosenthal, K., Dhariwal, G., Lee, J., and Chatterjee, D.K. (2002) The role of template-primer in protection of reverse transcriptase from thermal inactivation. *Nucleic Acids Res.* **30**, 3118–3129
32. Cote, M.L. and Roth, M.J. (2008) Murine leukemia virus reverse transcriptase: structural comparison with HIV-1 reverse transcriptase. *Virus Res.* **134**, 186–202
33. Patel, P.H., Jacobo-Molina, A., Ding, J., Tantillo, C., Clark, A.D., Jr, Raag, R., Nanni, R.G., Hughes, S.H., and Arnold, E. (1995) Insights into DNA polymerization mechanisms from structure and function analysis of HIV-1 reverse transcriptase. *Biochemistry* **34**, 5351–5363
34. Ding, J., Das, K., Hsiou, Y., Sarafianos, S.G., Clark, A.D., Jr, Jacobo-Molina, A., Tantillo, C., Hughes, S.H., and Arnold, E. (1998) Structure and functional implications of the polymerase active site region in a complex of HIV-1 RT with a double-strand DNA template-primer and an antibody Fab fragment at 2.8 Å resolution. *J. Mol. Biol.* **284**, 1095–1111
35. Pandey, P.K., Kaushik, N., Talele, T.T., Yadav, P.N.S., and Pandey, V.N. (2001) Insertion of a peptide from MuLV RT into the connection subdomain of HIV-1 RT results in a functionally active chimeric enzyme in monomeric conformation. *Mol. Cell. Biochem.* **225**, 135–144
36. Pandey, P.K., Kaushik, N., Singh, K., Sharma, B., Upadhyay, A.K., Kumar, S., Harris, D., and Pandey, V.N. (2002) Insertion of a small peptide of six amino acids into the β7-β8 loop of the p51 subunit of HIV-1 reverse transcriptase perturbs the heterdimer and affects its activities. *BMC Biochem.* **3**, 18
37. Yasukawa, K., Tsuchiya, S., Ekida, T., Iida, H., Ide, T., Miki, D., Yagame, H., Murayama, K., and Ishiguro, T. (2003) Fusion protein of interleukin-6 and interleukin-6 receptor without polypeptide linker. *J. Biosci. Bioeng.* **96**, 38–46
38. Yutani, K., Ogasahara, K., Tsujita, T., and Sugino, Y. (1987) Dependence of conformational stability on hydrophobicity of the amino acid residue in a series of variant proteins substituted at a unique position of tryptophan synthase α subunit. *Proc. Natl Acad. Sci. USA* **84**, 4441–4444
39. Shoichet, B.K., Baase, W.A., Kuroki, R., and Matthews, B.W. (1995) A relationship between protein stability and protein function. *Proc. Natl Acad. Sci. USA* **92**, 452–456
40. Lee, S., Oneda, H., Minoda, M., Tanaka, A., and Inouye, K. (2006) Comparison of starch hydrolysis activity and thermal stability of two *Bacillus licheniformis* α-amylase and insights into engineering α-amylase variants active under acidic conditions. *J. Biochem.* **139**, 997–1005
41. Lee, A., Mouri, Y., Minoda, M., Oneda, H., and Inouye, K. (2006) Comparison of the wild-type α-amylase and its variant enzymes in *Bacillus amyloliquefaciens* in activity and thermal stability, and insights into engineering the thermal stability of *Bacillus* α-amylase. *J. Biochem.* **139**, 1007–1015
42. Yasukawa, K. and Inouye, K. (2007) Improving the activity and stability of thermolysin by site-directed mutagenesis. *Biochim. Biophys. Acta* **1774**, 1281–1288
43. Takita, T., Aono, T., Sakurama, H., Itoh, T., Wada, T., Minoda, M., Yasukawa, K., and Inouye, K. (2008) Effects of introducing negative charges into the molecular surface of thermolysin by site-directed mutagenesis on its activity and stability. *Biochim. Biophys. Acta* **1784**, 481–488
44. Muller, B., Restle, T., Weiss, S., Gautel, M., Sczakiel, G., and Goody, R.S. (1989) Co-expression of the subunits of the heterodimer of HIV-1 reverse transcriptase in *Escherichia coli*. *J. Biol. Chem.* **264**, 13975–13978

Downloaded from http://jb.oxfordjournals.org/ at Islamic Azad University on September 28, 2012